Heliyon 10 (2024) e35197

Contents lists available at ScienceDirect

Heliyon

journal homepage: www.cell.com/heliyon

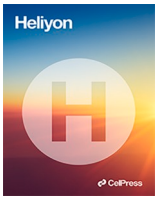

Research article

Macrophage-derived exosomal miR-155 regulating hepatocyte pyroptosis in MAFLD

Wei He [*,1], Jin Xu [1], Xiang Wang [**], Zhining Fan, Hai Li

Department of Gastroenterology, Geriatric Hospital of Nanjing Medical University, Jiangsu Province Geriatric Institute, Jiangsu Province Official Hospital, Nanjing, 210024, Jiangsu Province, China

A R T I C L E I N F O

Keywords:
Macrophage
Exosome
miR-155
Hepatocyte
Pyroptosis

A B S T R A C T

Background: Previous studies have shown that pyroptosis in hepatocyte is essential for the development of MAFLD. Growing evidence has shown that exosomal miRNAs-mediated communication between inflammatory cells and hepatocyte is an important link in MAFLD. In the present study, we aim to elucidate whether macrophage-derived exosomal miRNAs contribute to the hepatocyte pyroptosis in the pathophysiological process of MAFLD.

Methods: The effects of hepatocyte pyroptosis were investigated in an HFD-induced MAFLD mouse model and in the liver tissues from patients with MAFLD using immunohistochemistry, real-time PCR, Western blotting, and luciferase reporter assay, among other techniques. MiR-155 inhibitor tail injections and AAV-FoxO3a-GFP were also administered to respectively inhibit or overexpress its expression in an HFD-induced MAFLD mouse model.

Results: Hepatocyte pyroptosis was heightened in the liver tissue of patients with MAFLD or HFD-induced MAFLD mouse. Importantly, treatment with a caspase-1 inhibitor or overexpression of FoxO3a reversed this trend. Our study also demonstrated that miR-155 expression and the number of infiltrated macrophages were increased, and knockdown of miR-155 attenuated hepotocyte pyroptosis and liver fibrosis in HFD-induced mouse. In addition, we demonstrated that macrophage-derived exosomal miR-155 was transferred to hepatocytes, leading to hepatocyte pyroptosis in MAFLD mouse. Furthermore, blockade of exosome secretion improved hepotocyte pyroptosis and liver fibrosis in HFD-induced mouse. On the contrary, macrophage-derived exosomal miR-155 worsened hepotocyte pyroptosis. Moreover, we found that miR-155 promoted hepatocyte pyroptosis in MAFLD by down-regulating FoxO3a.

Conclusions: Taken together, our results demonstrated that macrophage-derived exosomal miR-155 promotes hepatocyte pyroptosis and liver fibrosis in MAFLD.

1. Introduction

Metabolic associated fatty liver disease (MAFLD), formerly known as nonalcoholic fatty liver disease (NAFLD), affects up to 25 % of

* Corresponding author. Department of Gastroenterology, Geriatric Hospital of Nanjing Medical University, Jiangsu Province Geriatric Institute, Jiangsu Province Official Hospital, Nanjing, 210024, Jiangsu Province, China.

** Corresponding author. Department of Gastroenterology, Geriatric Hospital of Nanjing Medical University, Jiangsu Province Geriatric Institute, Jiangsu Province Official Hospital, Nanjing, 210024, Jiangsu Province, China.

E-mail addresses: bingbing_he@yeah.net (W. He), wxnanjing@163.com (X. Wang).

[1] These authors contributed equally to this work.

https://doi.org/10.1016/j.heliyon.2024.e35197
Received 4 November 2023; Received in revised form 24 July 2024; Accepted 24 July 2024
Available online 25 July 2024

the global population, posing serious threats to human health and imposing substantial economic burdens on society [1,2]. In China, the incidence of MAFLD is rising rapidly, with a trend towards younger ages, and currently, the prevalence stands at approximately 15 % [3].

Pyroptosis is a form of programmed cell death that plays an important role in the onset and progression of liver diseases [4,5]. The classic pyroptosis pathway is mainly characterized by caspase 1 activation and cleavage of GSDMD to generate cleaved GSDMD (pyroptosis marker), which can perforate and kill the cell membrane, accompanied by the release of inflammatory factors such as IL-1β and IL-18 [6]. In recent years, numerous studies have shown that hepatocyte pyroptosis is an important link in the pathophysiological mechanism of MAFLD [7–9]. However, the mechanism of hepatocyte pyroptosis in MAFLD remains unclear at present and warrants further investigation.

FoxO (Forkhead transcription factor, O subfamily) factor is a subgroup of the Forkhead protein family, comprising FoxO1, FoxO3a, FoxO4, and FoxO6. As a type of transcription factor, FoxO protein binds to specific targets in the nucleus, initiating downstream gene transcription [10]. Down-regulated FoxO3a induces cardiomyocyte pyroptosis by activating the ASC/IL-1β signaling pathway in both diabetic and uremic cardiomyopathy [11,12]. In alcoholic liver disease, the down-regulation of FoxO1, a transcription factor of miR-148a, results in increased expression of TXNIP, a target gene of miR-148a. This ultimately leads to hepatocyte pyroptosis [13]. However, whether FoxO1, FoxO3a, or both are involved in hepatocyte pyroptosis in MAFLD remains largely unknown.

Exosomes are goblet shaped microvesicles secreted by cells with a diameter of about 30–130 nm, which carry miRNAs, long non-coding RNAs(lncRNAs), mRNAs and other substances that can mediate communication between different cells and tissues [14]. Growing evidence has demonstrated that exosome-mediated cellular crosstalk between hepatocyte and inflammatory cells contributed to the development of liver-related diseases including MAFLD, liver cancer, and liver fibrosis [15–17].

At the current study, we investigated the role of macrophage-derived exosomal miR-155 on the regulation of FoxO signaling and hepatocyte pyroptosis in the pathophysiological process of MAFLD.

2. Methods

2.1. Human liver samples

A total of 10 pathological liver samples from individuals with MAFLD were collected. Additionally, six normal liver tissue samples from patients with hepatic hemangioma without underlying hepatic diseases were obtained and used as negative controls. All patients were informed about the use of their specimens and signed an informed consent agreement. This study was reviewed and approved by the ethics committee of Jiangsu Province Official Hospital with the approval number: 2022-037, dated 2022 12 28. The study adhered to the principles outlined in the Declaration of Helsinki.

2.2. MAFLD mouse model and treatments

C57BL/6 wild-type male mice (22–25 g) were purchased from The Jackson Laboratory (Bar Harbor, ME,USA). The MAFLD mouse model was obtained through a high-fat diet (HFD) (protein, 18.1 %; fat, 61.6 %; and carbohydrates, 20.3 %; Jinpan biotechnology, Shanghai, China) for 10 weeks. Control group mice were fed a normal chow (NC) diet (protein, 18.3 %; fat, 10.2 %; and carbohydrates, 71.5 %; Tuopu biotechnology, Shenzhen, China). Ac-YVAD-cmk in DMSO (5 % v/v) was injected intraperitoneally to inhibit caspase-1 activity in MAFLD mice (once a week for 4 weeks before terminal). MAFLD mice were injected with a type 9 recombinant AAV-FoxO3a-GFP (1×10^{11} virion particles in 100 mL of saline solution) through the tail vein. MiR-155 inhibitor (Genechem Biotech Inc) combining with In vivo-jetPEITM (Polyplus-transfection, New York, USA) were used to deliver miR-155 inhibitor into the liver via tail injection in MAFLD mice (twice at two-day intervals for the last 4 weeks before terminal). All animal experiments were approved by the Institutional Animal Care and Use Committee of Nanjing Medical University(IACUC-2101016).

2.3. Morphologic analysis and immunohistochemistry

3 μm sections of the formalin-fixed, paraffin-embedded liver were prepared for Masson's trichrome staining and immunohistochemical stains. The primary antibodies against caspase-1 (1:200), FoxO1 (1:200), FoxO3a (1:200), IL-1β (1:200), IL-18 (1:200), and GSDMD (1:200) in PBS containing 3 % bovine serum albumin. Horseradish-peroxidase coupled secondary antibodies (Vectastain elite, Vector Labs) were used for staining. All immunohistochemical analyses were repeated at least three times and representative images were presented.

2.4. Terminal deoxynucleotidyl transferase dUTP nick-end labeling (TUNEL) staining

TUNEL staining was performed using an in situ apoptosis detection kit (Takara Bio Inc., Tokyo, Japan) to detect cell death.

2.5. Isolation of hepatocyte, HSC, and macrophage in mouse liver tissues

Primary liver cells were isolated from 8-week-old male C57BL/6J wild-type mice. The liver was perfused with digestion solutions containing pronase and collagenase IV. Hepatocytes were isolated and cultured as previously described [18,19]. The liver was collected and transferred into a 10 cm dish containing cold HBSS-CaCl2 buffer after the perfusion was completed.Cut the liver until all

the large clumps are removed, and then the cells were filtered through a 70 μm cell strainer using cold HBSS-CaCl2 buffer. Centrifuge at a speed of 50 g at 4 °C for 3 min. Discard the supernatant and collect the sediment. HSCs were separated from non-parenchymal cells (NPCs) using a reported method [20,21]. Generally, the supernatants of NPCs were centrifuged at 450 g at 4 °C for 10 min. Then, the cell sediment was collected and centrifuged on a Nycodenz cushion at 1400×*g* for 15 min. The supernatant was collected, and subsequent centrifugation generated the HSCs. Kuffer cells were isolated by perfusion in situ [22,23]. The liver was dispersed gently, and the cell suspension was centrifuged at 50 g for 5 min. The supernatants were collected and then centrifuged again at 50 g for 5 min. The cell sediment was collected and resuspended using 25 % Percoll, and then added into 50 % Percoll and centrifuged at 800 g for 20 min. The Kuffer cells were collected from the interface between the 25 % Percoll and 50 % Percoll layers.

2.6. Exosome purification from liver tissues

Briefly, the liver tissue was cut into uniform pieces of 1 m^3, homogenized and filtered. Then, the supernatant was centrifuged at 2000×*g* for 15 min, 16,000×*g* for 30 min, and 160,000×*g* for 180 min. The exosome pellets were re-suspended in PBS and stored at −80 °C.

2.7. Exosome transfusion experiment

As described previously, RAW264.7 cells were cultured in FBS-free DMEM for 48 h, and then the conditioned medium was collected. The extracellular vesicles were purified through several centrifugation and filtration steps. Saline or exosomes derived from RAW264.7 (100 mg) were injected intraperitoneally into MAFLD mice twice per week for a total of 4 weeks before the mice were sacrificed.

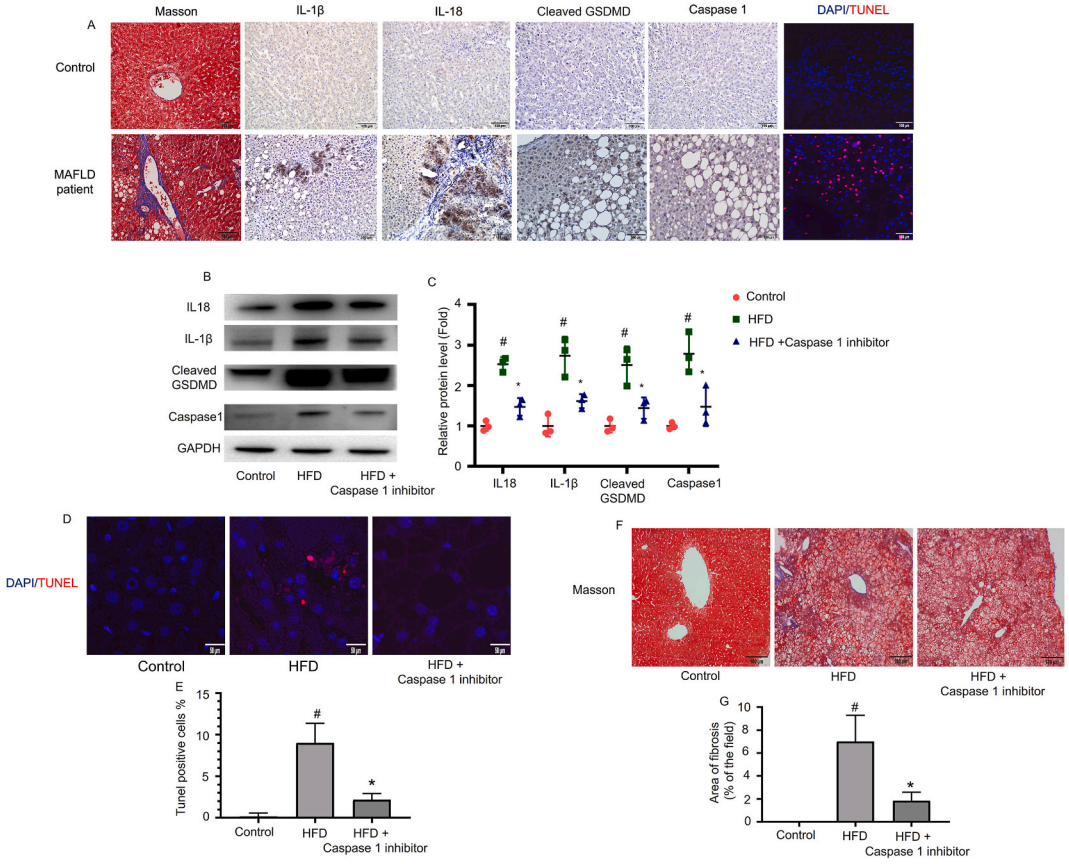

Fig. 1. Hepatocytes pyroptosis contributes to the development of MAFLD. (A) Representative Masson staining and immunohistochemical staining of Caspase 1, IL-1β, IL-18, and GSDMD, as well as TUNEL assay in the liver tissues from MAFLD patients or normal control. (B)Western blot analysis revealed the expression of the level of Caspase 1, IL-1β, IL-18, and Cleaved GSDMD in the liver tissues from various groups as indicated. (C) Graphical presentation shows the relative abundance levels of Caspase 1, IL-1β, IL-18, and Cleaved GSDMD after normalization with GAPDH in Fig. 1B. (D) The TUNEL assay in liver sections from various groups as indicated. (E) Quantification of TUNEL-positive hepatocytes in Fig. 1D. (F) Representative Masson staining in liver sections from various groups as indicated. (G) Semi-quantification of the Trichrome-positive area in Fig. 1F. #P < 0.05 versus control, *P < 0.05 versus HFD group.

2.8. Western blot analysis

Cells harvested from liver tissues and plates were lysed in RIPA buffer. The membranes were blocked with 5 % bovine serum albumin and subsequently incubated with primary antibodies, including caspase-1 (1:1000, Abcam, Cambridge, MA), IL-1β (1:1000, Abcam, Cambridge, MA), IL-18 (1:1000, Santa Cruz Biotechnology, TX), FoxO1 (1:1000, Cell Signaling Technology, MA), FoxO3a (1:1000, Cell Signaling Technology, MA); GSDMD (1:1000, Abcam, Cambridge, MA), and GAPDH (1:5000, CMCTAG, WI). Then, the membranes were washed three times with TBS-T for 30 min and incubated with secondary antibody. The bands were detected and analyzed using the ChemiDoc XRS System.

2.9. Real-time PCR

RNA enriched in small RNAs was extracted from the exosomes and liver tissues for miRNA profile analysis using a mirVana miRNA isolation kit (Ambion, Austin, TX, USA). The expression of pri-miRNA and miRNA was measured as previously described [24].

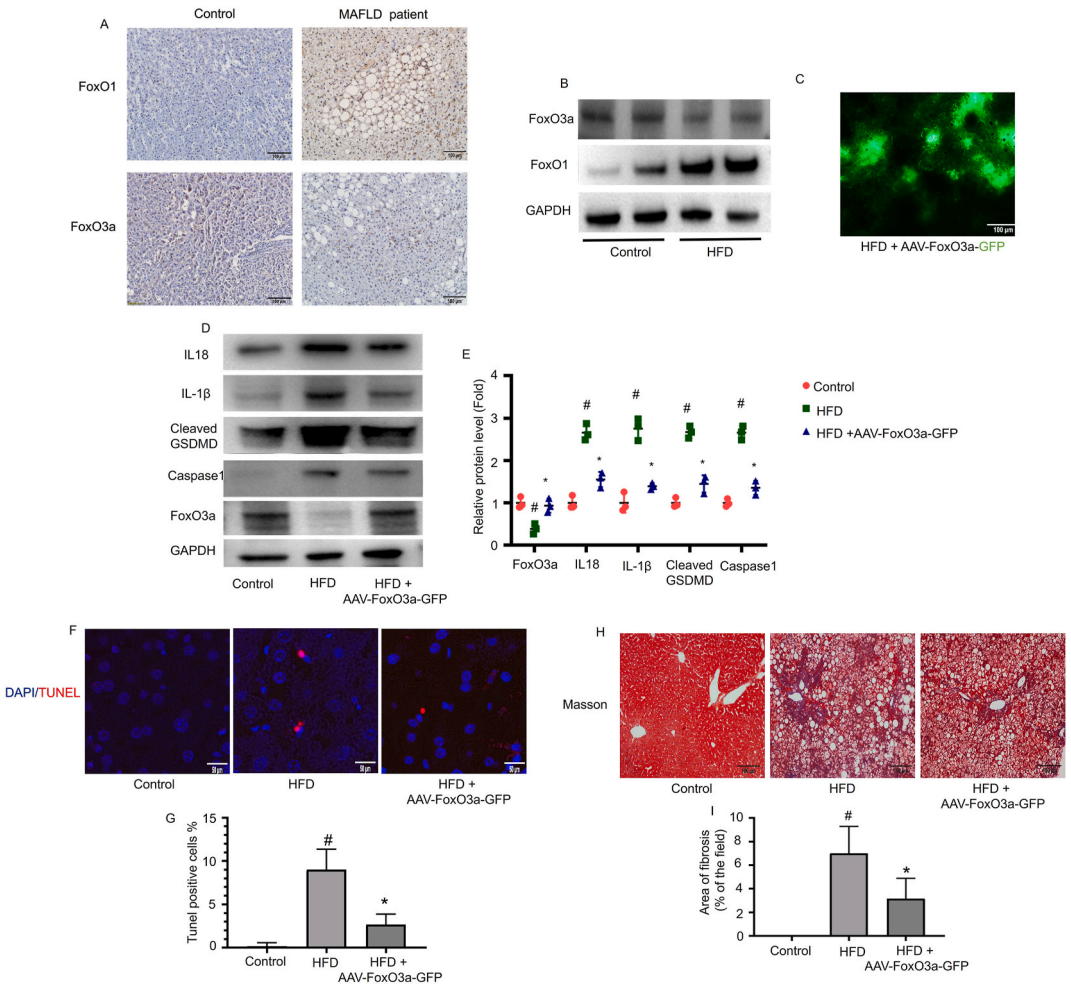

Fig. 2. FoxO3a down-regulation led to hepatocytes pyroptosis and liver fibrosis in MAFLD. (A) Representative immunohistochemical staining of FoxO1 and FoxO3a in the liver tissues from MAFLD patients or normal control. (B) Western blot analysis revealed the expression of the level of FoxO1 and FoxO3a in the liver tissues of mouse from various groups as indicated. (C) Green fluorescence indicates AAV9-FoxO3a-GFP infected liver tissues. (D)Western blot analysis revealed the expression of the level of Caspase 1, IL-1β, IL-18, Cleaved GSDMD, and FoxO3a in the liver tissues from various groups as indicated. (E) Graphical presentation shows the relative abundance levels of Caspase 1, IL-1β, IL-18, Cleaved GSDMD, and FoxO3a after normalization with GAPDH in Fig. 1D. (F) The TUNEL assay in liver sections from various groups as indicated. (G) Quantification of TUNEL-positive hepatocytes in Fig. 1F. (H) Representative Masson staining in liver sections from various groups as indicated. (I) Semi-quantification of the Trichrome-positive area in Fig. 1H. #P < 0.05 versus control, *P < 0.05 versus HFD group.

2.10. Luciferase reporter assay and transfection

The FoxO3a 3′UTR containing the putative or mutated miR-155–5p binding sites was cloned into a luciferase reporter plasmid (pMIR-REPORT Luciferase), which was purchased from Applied Biosystems (Waltham, MA, USA). The constructs were co-transfected with miR-155 mimic or miR-155 inhibitor into 293T cells for 48 h. The enzymatic activities of firefly and Renilla luciferases were sequentially measured using a dual luciferase assay and a luminometer (Turner Designs, Sunnyvale, CA, USA).

2.11. Statistical analyses

All data were presented as the mean ± standard error of mean (SEM). Student's t-test was performed to compare data between the two groups. For comparisons between multiple groups, one-way analysis of variance (ANOVA) followed by Dunnett's multiple comparison test was applied. Statistical analyses were carried out with Prism 7.0 (GraphPad Software, San Diego, California).

3. Results

1. Hepatocyte pyroptosis is induced in MAFLD

To firstly identify pyroptosis in hepatocyte is involved in MAFLD, we examined pyroptosis markers in liver tissues from MAFLD patients. As shown in Fig. 1A, the expression of cleaved GSDMD, caspase 1, IL-18 and IL-1β as well as the TUNEL-labeled hepatocyte

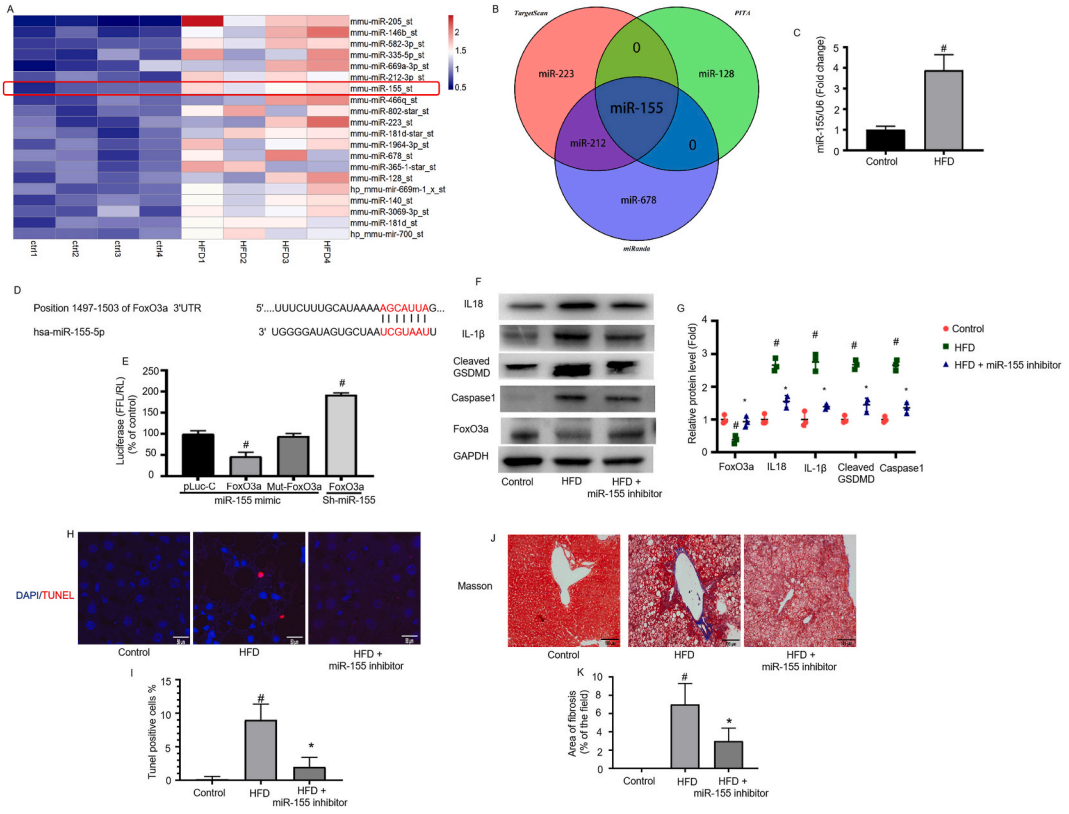

Fig. 3. MiR-155 regulates hepotocyte pyroptosis and liver fibrosis via targeting FoxO3a 3′-UTR in MAFLD. (A) Sequencing analysis of miRNA from GEO database (GSE65978) showed the top 20 significantly upregulated miRNAs in HFD group compared with the control group. (B) Among the top 20 miRNAs significantly upregulated, TargetScan, Pita, and miRanda jointly predicted the targeted regulation of FoxO3a gene by miR-155. (C) qRT-PCR results for miR-155 in the liver tissues of mouse from various groups as indicated. (D) Schematic of human FoxO3a 3′UTRs. Locations of the predicted miR-155a-binding sites are indicated. (E) Relative luciferase activity in 293T cells transfected with reporter constructs containing the 3′UTRs of target genes and cotransfected with miR-155 mimics or negative control (NC) or sh-miR-155 (miR-155 inhibitor). Mut, mutant. #p < 0.05 vs. mimic control. (F) Western blot analysis revealed the expression of the level of Caspase 1, IL-1β, IL-18, Cleaved GSDMD, and FoxO3a in the liver tissues from various groups as indicated. (G) Graphical presentation shows the relative abundance levels of Caspase 1, IL-1β, IL-18, Cleaved GSDMD, and FoxO3a after normalization with GAPDH in Fig. 1F. #P < 0.05 versus control, *P < 0.05 HFD group. (H) The TUNEL assay in liver sections from various groups as indicated. (I) Quantification of TUNEL-positive hepatocytes in Fig. 1H. (J) Representative Masson staining in liver sections from various groups as indicated. (K) Semi-quantification of the Trichrome-positive area in Fig. 1J. #P < 0.05 versus control, *P < 0.05 versus HFD group.

death were significantly increased in liver tissue of MAFLD compared with the healthy controls. Similar to the human samples, pyroptosis was also induced in liver tissue of HFD-induced MAFLD mouse model (Fig. 1B and E). More importantly, caspase-1 inhibitor treatment ameriorated hepatocyte pyroptosis and liver fibrosis in HFD-induced animal mouse model (Fig. 1B through 1G). Collectively, the above results suggested that pyroptosis is involved in the development of MAFLD.

2. FoxO3a, but not FoxO1, negatively regulated hepatocyte pyroptosis in HFD-induced mice.

Since FoxO family proteins mainly play a negative role in regulating cell pyroptosis in liver as well as other organs [13,25–27], and FoxO1 and FoxO3a are the main two isforms in the liver. We speculated that downregulation of FoxO1 and/or FoxO3a may be involved in hepatocyte pyroptosis in MAFLD. Interestingly, the expression of FoxO3a protein was indeed decreased, whereas FoxO1 protein was increased in MAFLD patients compared with the control group (Fig. 2A). Similarly, FoxO3a and FoxO1 showed the same tendency in HFD-induced mouse compared with the control mouse (Fig. 2B). Therefore, we overexpressed FoxO3a in the liver of MAFLD mice using AAV-FoxO3a-GFP (Fig. 2C). As expected, hepatocyte pyroptosis was significantly attenuated after AAV-FoxO3a-GFP treatment, as indicated by the downregulation of GSDMD-N, IL-18, and IL-1β, as well as TUNEL-labeled hepatocyte death (Fig. 2D through 2G). In addition, AAV-FoxO3a treatment improved liver fibrosis in the HFD-induced MAFLD mouse model (Fig. 2H and I). Of note, minimal changes in FoxO3a mRNA level were found in the liver tissue of MAFLD mice relative to control group (Supplemental Fig. 1).

3. Inhibiting miR-155 expression attenuated hepatocyte pyroptosis hepatocyte pyroptosis and fibrosis by targeting FoxO3a 3′-UTR

Because MicroRNAs (miRs) have also been shown to cause cellular pyroptosis through FoxO regulation in the liver and other organs [12,13], we mainly focus the role of miRs in regulating hepatocyte FoxO3a expression and pyroptosis under MAFLD condition. Data from GEO database indicated that 5 miRNAs (miR-155, miR-223, miR-128, miR-212, miR-678) were predicted to target FoxO3a gene

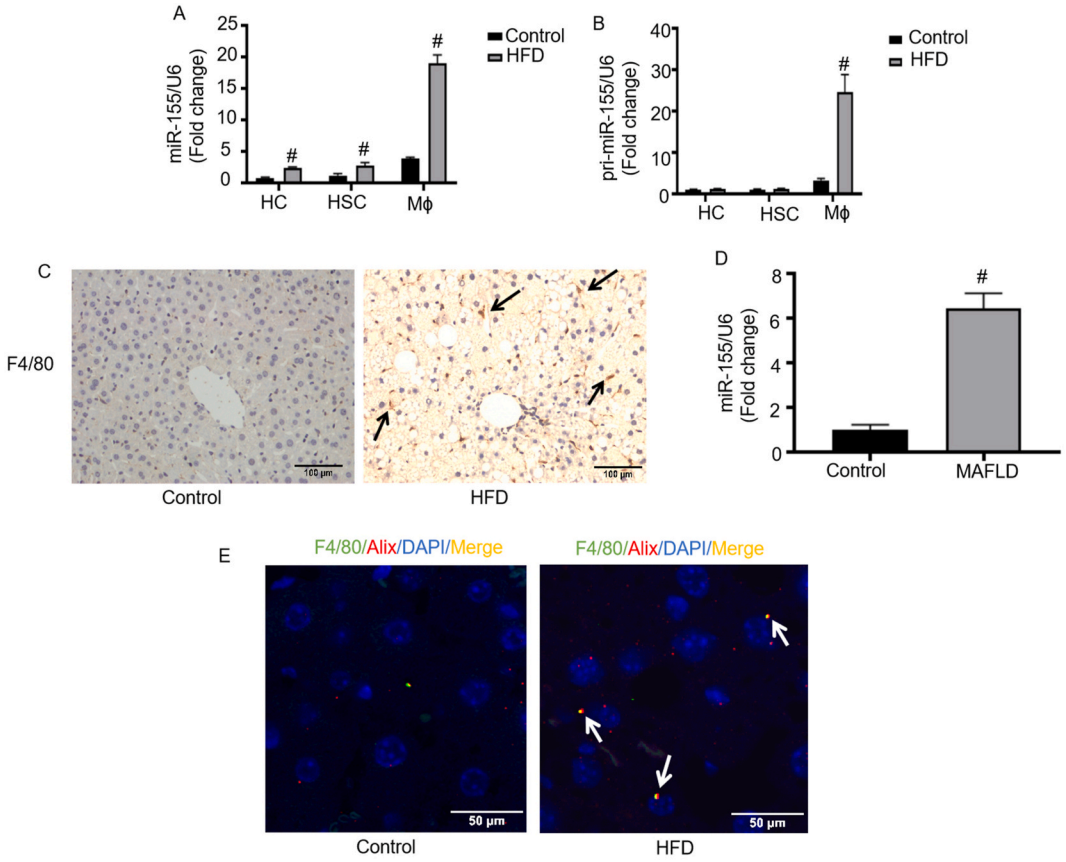

Fig. 4. Macrophage derived exosomal miR-155 was transferred into hepatocytes in HFD-induced MAFLD mouse. (A). qRT-PCR analysis of miR-155 and (B) pri-miR-155 relative folds to U6 expression in hepatocyte (HC), Hepatic stellate cells (HSC), and macrophages (Mϕ) isolated from the control and MAFLD mouse is shown. (C) Representative immunohistochemical staining of F4/80 in control and MAFLD liver tissues. (D) qRT-PCR analysis of miR-155 relative folds to U6 expression in the exosomes harvested from the control and MAFLD liver tissues. (E) Representative images demonstrating the expression and localization of F4/80 (green), Alix (red), and DAPI (blue) by indirect immunofluorescent staining in sections of livers from mouse in each group, as indicated. #P < 0.05 versus control.

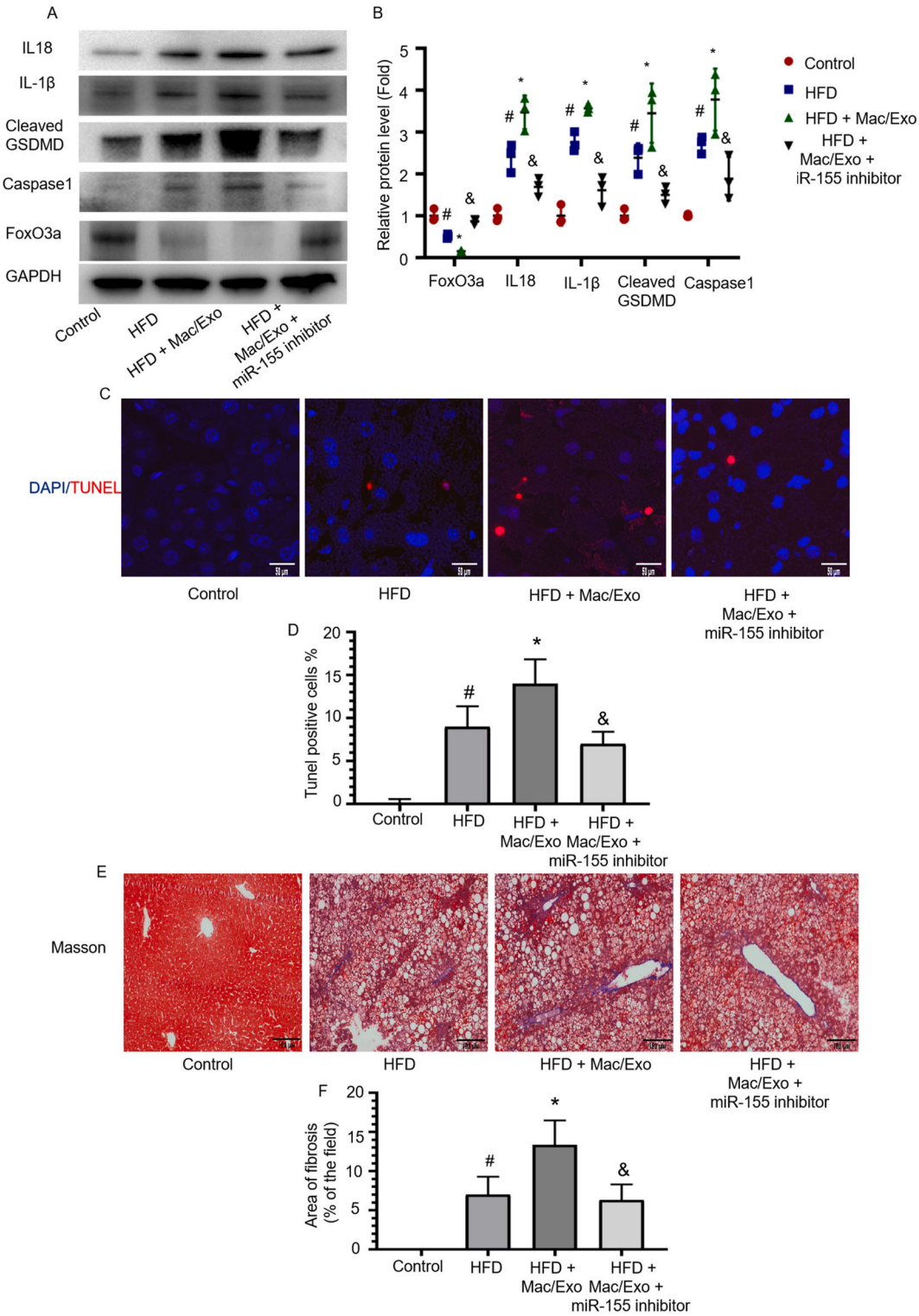

Fig. 5. Macrophage-derived exosome enhanced hepatocyte pyroptosis and fibrosis via transferring miR-155 into hepatocytes in HFD-induced MAFLD mouse. (A)Western blot analysis revealed the expression of the level of Caspase 1, IL-1β, IL-18, Cleaved GSDMD, and FoxO3a in the liver tissues from various groups as indicated. (B) Graphical presentation shows the relative abundance levels of Caspase 1, IL-1β, IL-18, Cleaved GSDMD, and FoxO3a after normalization with GAPDH in Fig. 1A. (C) The TUNEL assay in liver sections from various groups as indicated. (D) Quantification of TUNEL-positive hepatocytes in Fig. 1C. (E) Representative Masson staining in liver sections from various groups as indicated. (F) Semi-quantification of the Trichrome-positive area in Fig. 1E. #P < 0.05 versus control, *P < 0.05 versus HFD group.

among the top 20 up-regulated miRNAs in liver tissue of MAFLD mouse model induced by HFD. However, only miR-155 was predicted to target FoxO3a gene by TargetScan, Pita, and miRanda (Fig. 3A and B). In our further verifying experiment, the expression level of miR-155 in the liver tissue of MAFLD mice was 3.9 times higher than that of the control group (Fig. 3C). Moreover, miR-155 was predicted to recognize sites 1497–1503 in the 3′-UTR region of FoxO3a (Fig. 3D), and the lucifeance reporter gene results confirmed that miR-155 could negatively regulate the expression of FoxO3a gene by binding to this site (Fig. 3E). More importantly, miR-155 inhibitor treatment significantly restored hepatocyte FoxO3a expression and attenuated hepatocyte pyroptosis, resulting in the ameliorated of liver fibrosis in the HFD-induced MAFLD mouse model (Fig. 3F through 3K).

4. Macrophage derived exosomes transferred miR-155 into hepatocytes in HFD-induced MAFLD mouse model

It is well known that miR-155 is an inflammation-related miRNA, primarily expressed in macrophages and other inflammatory cells [27]. In the MAFLD mouse model, the expression levels of miR-155 in hepatocytes, hepatic stellate cells (HSCs), and macrophages were 2.9, 4.6, 5.5 times higher than those in the control group, respectively (Fig. 4A). In the MAFLD mouse model, the pri-miR-155 was not significantly increased in hepatocytes and hepatic stellate cells compared with the control mouse (Fig. 4B). However, the expression level of pri-miR-155 in macrophages from liver tissue of MAFLD mice was 7.5-fold higher than that of the control group (Fig. 4B). Immunohistochemical results showed that the infiltration of F4/80-positive macrophages in the liver tissue of MAFLD mice was significantly increased compared to control mouse (Fig. 4C). In addition, the expression level of miR-155 in the exosomes of liver tissue

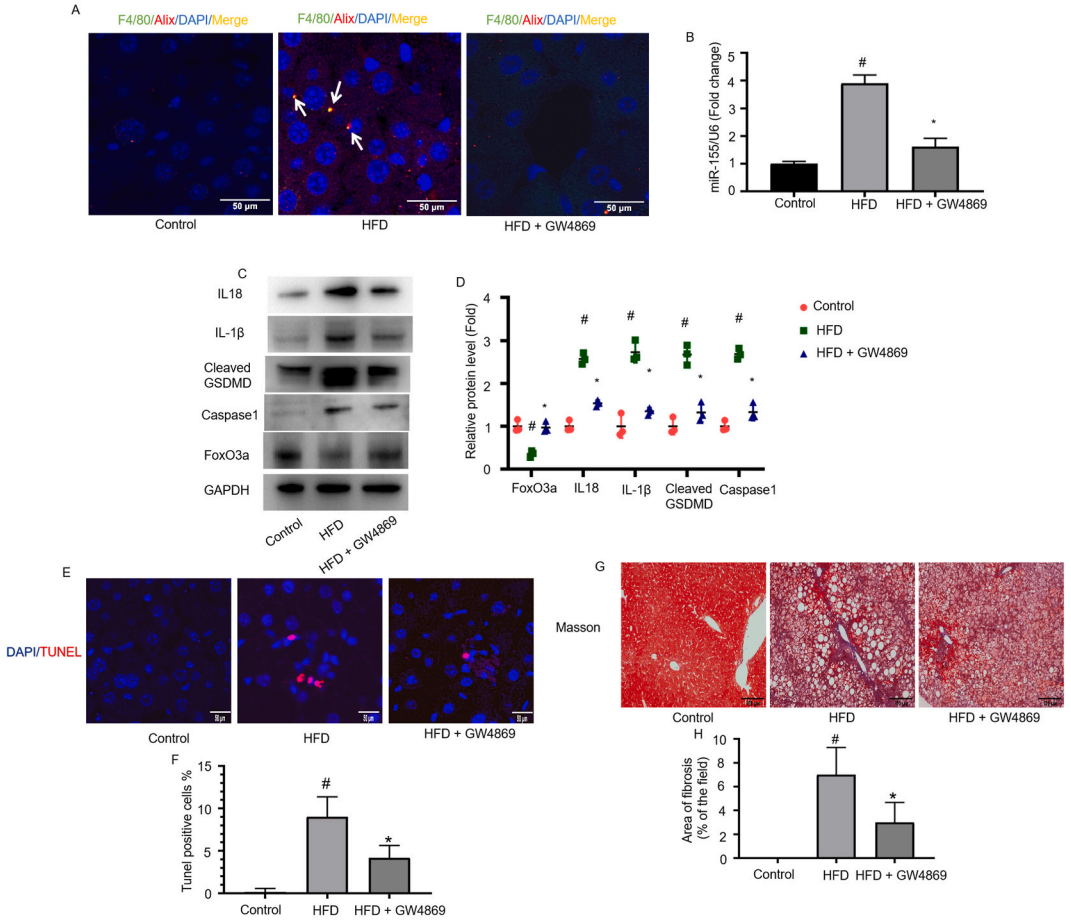

Fig. 6. Blockade of exosome secretion with GW4869 attenuated hepatocyte pyroptosis and liver fibrosis in HFD-induced MAFLD mouse. (A) Representative images demonstrating the expression and localization of F4/80 (green), Alix (red), and DAPI (blue) by indirect immunofluorescent staining in sections of livers from mouse in each group, as indicated. (B) qRT-PCR analysis of miR-155 relative folds to U6 expression in the exosomes harvested from the control and MAFLD liver tissues. (C)Western blot analysis revealed the expression of the level of Caspase 1, IL-1β, IL-18, Cleaved GSDMD, and FoxO3a in the liver tissues from various groups as indicated. (D) Graphical presentation shows the relative abundance levels of Caspase 1, IL-1β, IL-18, Cleaved GSDMD, and FoxO3a after normalization with GAPDH in Fig. 1C. (E) The TUNEL assay in liver sections from various groups as indicated. (F) Quantification of TUNEL-positive hepatocytes in Fig. 1E. (G) Representative Masson staining in liver sections from various groups as indicated. (H) Semi-quantification of the Trichrome-positive area in Fig. 1G. #P < 0.05 versus control, *P < 0.05 versus HFD group.

of MAFLD mice was 6.35-fold higher than that of the control group (Fig. 4D). Furthermore, F4/80 (Macrophages marker)/Alix (Exosome marker) colocationed signal was increased in hepatocyte in the HFD-induced MAFLD mouse model (Fig. 4E). Collectively, all the above results indicated that macrophage-derived exosomes could transfer miR-155 into hepatocytes in the HFD-induced MAFLD mouse model.

5. Macrophage derived exosome enhanced hepatocyte pyroptosis and fibrosis via transferring miR-155 into hepatocytes in HFD-induced MAFLD mouse model

To further confirm the role of macrophage-derived exosomal miR-155 in regulating hepatocytes pyroptosis and liver fibrosis processes, we injected macrophage-derived exosomes into HFD-induced MAFLD mouse. Interestingly, macrophage-derived exosome enhanced hepatocytes pyroptosis and worsened the liver fibrosis in HFD-induced MAFLD mouse model, which was attenuated by miR-155 inhibitor treatment (Fig. 5). Taken together, our results suggested that macrophage-derived exosome transferred miR-155 into hepatocytes and enhanced hepatocyte pyroptosis and fibrosis in MAFLD.

6. Blocking exosome secretion with GW4869 attenuated hepatocytes pyroptosis and fibrosis in HFD-induced MAFLD mouse model

GW4869 is the most widely used pharmacologic agent for blocking exosome generation. Firstly, the colocalization signal of F4/80 and Alix was decreased in hepatocyte compared to that in the HFD-induced MAFLD mouse model (Fig. 6A). In addition, the expression level of miR-155 in the exosomes of liver tissue of MAFLD mice was lower than HFD-induced MAFLD mouse (Fig. 6B). Of note, GW4869 treatment abrogated hepatocytes pyroptosis and liver fibrosis compared with the HFD group (Fig. 6C through 6H).

4. Discussion

In our current study, we firstly illustrated that macrophage-derived exosomal miR-155 worsened hepatocyte pyroptosis by down-regulating FoxO3a protein expression in MAFLD, as summarized in Fig. 7.

In MAFLD, the traditional "second hit hypothesis" posits that the initial "hit" is hepatic steatosis, which leads to mitochondrial dysfunction in hepatocytes and increases the liver's vulnerability to a subsequent attack. The second "hit" involves lipid peroxidation and an increased production of reactive oxygen species, ultimately resulting in liver cell damage, inflammation, and fibrosis [28]. In recent years, the "multiple blow hypothesis" has been gradually accepted, suggesting that various factors contributing to liver cell injury occur simultaneously rather than in a simple sequential manner [29]. Theoretically, all factors exacerbating MAFLD injury represent potential therapeutic targets. Therefore, investigating the pathophysiological mechanisms underlying liver cell injury in MAFLD is of great significance for the prevention and treatment of the disease.

Taurine can alleviate As2O3-induced non-alcoholic steatohepatitis by inhibiting NLRP3 inflammasome activation and hepatocyte pyroptosis [30]. A previous study have confirmed that inflammasome proteins released by hepatocyte pyroptosis can promote the

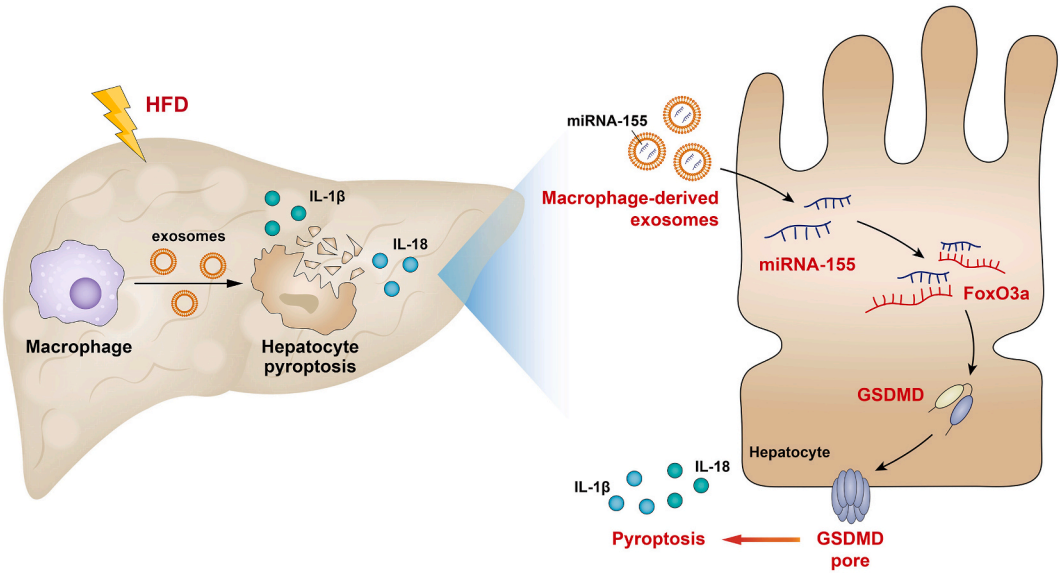

Fig. 7. Working model of macrophage-derived exosomal miR-155 induced hepatocyte pyroptosis and liver fibrosis via down-regulating FoxO3a expression in MAFLD. Under MAFLD condition, macrophages infiltration and macrophage-derived exosomal miR-155 loading were significantly increased in the liver. The macrophage released exosomal miR-155 was transferred into the cytosol led to the translational repression of FoxO3a in hepatocyte. Finally, macrophage-derived miR-155-containing exosomes promoted hepatocyte pyroptosis by directly targeting FoxO3a in MAFLD.

activation of stellate cells and the occurrence of liver fibrosis in MAFLD [9]. In the present study, we firstly identified that pyroptosis is involve in the development of MAFLD using human liver tissues and animal models, which is consistant with previous studies [7,9]. Hence, a deep understanding of the exact mechanism regulating hepatocyte pyroptosis is vital to develop new strategies to cure MAFLD.

Down-regulated FoxO3a induces cardiomyocyte pyroptosis in both diabetic and uremic cardiomyopathy [11,12]. In alcoholic liver disease, down-regulated expression of FoxO1 ultimately leads to hepatocyte pyroptosis [13]. In our study, FoxO1 is increased in MAFLD, which is consistant with previous studies. Therefore, hepatocyte pyroptosis is more likely due to the decreased expression of FoxO3a, rather than FoxO1, in MAFLD. Treatment with AAV-FoxO3a improved hepatocyte pyroptosis, confirming this point.

It is well known that miR-155 is an inflammation-related miRNA, primarily expressed in macrophages and other inflammatory cells [27]. As we all know, the increased infiltration of macropahges is a basic characteristic of MAFLD. Previous studies have also shown that macrophages play a crucial role in promoting the progression of MAFLD [31]. Furthermore, the interaction between macrophages and liver cells contributes to the onset and development of alcoholic liver disease, MAFLD, liver cancer, and other diseases [32–34]. Research has indicated that in MAFLD, exosomes released by lipotoxic liver cells deliver miR-192a to macrophages, activating macrophage polarization in liver tissue via the Rictor/Akt/FoxO1 signaling pathway and thus facilitating the progression of MAFLD [15]. Recent studies in models of alcoholic liver disease have also demonstrated that miR-155 can increase exosome secretion from liver cells and macrophages by suppressing the expression of the LAMP1 and LAMP2 genes [35,36]. In our results, we identified that the increased infiltrated macrophage derived exosomal miR-155 worsened hepatocytes pyroptosis via targeting FoxO3a in MAFLD.

In conclusion, macrophage-derived exosomes carrying miR-155 contribute to hepatocyte pyroptosis and the development of MAFLD. Inhibiting exosome-mediated crosstalk between macrophages and hepatocytes provides a new theoretical basis for the prevention and control of MAFLD.

Data availability statement

Data included in article.

CRediT authorship contribution statement

Wei He: Writing – review & editing, Writing – original draft, Funding acquisition, Data curation, Conceptualization. **Jin Xu:** Writing – review & editing, Software, Data curation. **Xiang Wang:** Supervision, Software, Methodology, Investigation, Conceptualization. **Zhining Fan:** Visualization, Project administration, Methodology, Investigation. **Hai Li:** Resources, Project administration, Data curation.

Declaration of competing interest

The authors declare that they have no known competing financial interests or personal relationships that could have appeared to influence the work reported in this paper.

Acknowledgments

This work was supported by grants from the National Natural Science Foundation of China (82100615) to Wei He.

Appendix A. Supplementary data

Supplementary data to this article can be found online at https://doi.org/10.1016/j.heliyon.2024.e35197.

References

[1] M. Eslam, A.J. Sanyal, J. George, MAFLD: a Consensus-Driven proposed nomenclature for metabolic associated fatty liver disease, Gastroenterology 158 (7) (2020) 1999–2014.
[2] Z.M. Younossi, A.B. Koenig, D. Abdelatif, Y. Fazel, L. Henry, M. Wymer, Global epidemiology of nonalcoholic fatty liver disease-Meta-analytic assessment of prevalence, incidence, and outcomes, Hepatology 64 (1) (2016) 73–84.
[3] J.Z. Zhu, Q.Y. Zhou, Y.M. Wang, Y.N. Dai, J. Zhu, C.H. Yu, et al., Prevalence of fatty liver disease and the economy in China: a systematic review, World J. Gastroenterol. 21 (18) (2015) 5695–5706.
[4] J. Wu, S. Lin, B. Wan, B. Velani, Y. Zhu, Pyroptosis in liver disease: new insights into disease mechanisms, Aging Dis 10 (5) (2019) 1094–1108.
[5] J. Gautheron, G.J. Gores, C. Rodrigues, Lytic cell death in metabolic liver disease, J. Hepatol. 73 (2) (2020) 394–408.
[6] X. Liu, Z. Zhang, J. Ruan, Y. Pan, V.G. Magupalli, H. Wu, et al., Inflammasome-activated gasdermin D causes pyroptosis by forming membrane pores, Nature 535 (7610) (2016) 153–158.
[7] J.I. Beier, J.M. Banales, Pyroptosis: an inflammatory link between NAFLD and NASH with potential therapeutic implications, J. Hepatol. 68 (4) (2018) 643–645.
[8] B. Xu, M. Jiang, Y. Chu, W. Wang, D. Chen, X. Li, et al., Gasdermin D plays a key role as a pyroptosis executor of non-alcoholic steatohepatitis in humans and mice, J. Hepatol. 68 (4) (2018) 773–782.
[9] S. Gaul, A. Leszczynska, F. Alegre, B. Kaufmann, C.D. Johnson, L.A. Adams, et al., Hepatocyte pyroptosis and release of inflammasome particles induce stellate cell activation and liver fibrosis, J. Hepatol. 74 (1) (2021) 156–167.

[10] A.E. Webb, A. Brunet, FOXO transcription factors: key regulators of cellular quality control, Trends Biochem. Sci. 39 (4) (2014) 159–169.
[11] X. Li, N. Du, Q. Zhang, J. Li, X. Chen, X. Liu, et al., MicroRNA-30d regulates cardiomyocyte pyroptosis by directly targeting foxo3a in diabetic cardiomyopathy, Cell Death Dis. 5 (2014) e1479.
[12] B. Wang, Z.M. Wang, J.L. Ji, W. Gan, A. Zhang, H.J. Shi, et al., Macrophage-Derived exosomal mir-155 regulating cardiomyocyte pyroptosis and hypertrophy in uremic cardiomyopathy, JACC Basic Transl. Sci. 5 (2) (2020) 148–166.
[13] M.J. Heo, T.H. Kim, J.S. You, D. Blaya, P. Sancho-Bru, S.G. Kim, Alcohol dysregulates miR-148a in hepatocytes through FoxO1, facilitating pyroptosis via TXNIP overexpression, Gut 68 (4) (2019) 708–720.
[14] H. Valadi, K. Ekstrom, A. Bossios, M. Sjostrand, J.J. Lee, J.O. Lotvall, Exosome-mediated transfer of mRNAs and microRNAs is a novel mechanism of genetic exchange between cells, Nat. Cell Biol. 9 (6) (2007) 654–659.
[15] X.L. Liu, Q. Pan, H.X. Cao, F.Z. Xin, Z.H. Zhao, R.X. Yang, et al., Lipotoxic Hepatocyte-Derived exosomal MicroRNA 192-5p activates macrophages through Rictor/Akt/Forkhead box transcription factor o1 signaling in nonalcoholic fatty liver disease, Hepatology 72 (2) (2020) 454–469.
[16] L. Fabris, K. Sato, G. Alpini, M. Strazzabosco, The tumor microenvironment in cholangiocarcinoma progression, Hepatology 73 (Suppl 1) (2021) 75–85.
[17] E. Kostallari, S. Valainathan, L. Biquard, V.H. Shah, P.E. Rautou, Role of extracellular vesicles in liver diseases and their therapeutic potential, Adv. Drug Deliv. Rev. 175 (2021) 113816.
[18] J.Y. Ge, Y.W. Zheng, T. Tsuchida, K. Furuya, H. Isoda, H. Taniguchi, et al., Hepatic stellate cells contribute to liver regeneration through galectins in hepatic stem cell niche, Stem Cell Res. Ther. 11 (1) (2020) 425.
[19] X.Y. Pan, H.M. You, L. Wang, Y.H. Bi, Y. Yang, H.W. Meng, et al., Methylation of RCAN1.4 mediated by DNMT1 and DNMT3b enhances hepatic stellate cell activation and liver fibrogenesis through Calcineurin/NFAT3 signaling, Theranostics 9 (15) (2019) 4308–4323.
[20] S. Lefere, T. Puengel, J. Hundertmark, C. Penners, A.K. Frank, A. Guillot, et al., Differential effects of selective- and pan-PPAR agonists on experimental steatohepatitis and hepatic macrophages, J. Hepatol. 73 (4) (2020) 757–770.
[21] E. Gonzalez-Sanchez, D. Firrincieli, C. Housset, N. Chignard, Expression patterns of nuclear receptors in parenchymal and non-parenchymal mouse liver cells and their modulation in cholestasis, Biochim. Biophys. Acta, Mol. Basis Dis. 1863 (7) (2017) 1699–1708.
[22] J.K. Park, M. Shao, M.Y. Kim, S.K. Baik, M.Y. Cho, T. Utsumi, et al., An endoplasmic reticulum protein, Nogo-B, facilitates alcoholic liver disease through regulation of kupffer cell polarization, Hepatology 65 (5) (2017) 1720–1734.
[23] W. Shi, Y. Wang, C. Zhang, H. Jin, Z. Zeng, L. Wei, et al., Isolation and purification of immune cells from the liver, Int. Immunopharm. 85 (2020) 106632.
[24] W. He, W. Ni, L. Zhao, X. Wang, L. Liu, Z. Fan, MicroRNA-125a/VDR axis impaired autophagic flux and contributed to fibrosis in a CCL4-induced mouse model and patients with liver cirrhosis, Life Sci. 264 (2021) 118666.
[25] S. Xu, J. Wang, J. Zhong, M. Shao, J. Jiang, J. Song, et al., CD73 alleviates GSDMD-mediated microglia pyroptosis in spinal cord injury through PI3K/AKT/Foxo1 signaling, Clin. Transl. Med. 11 (1) (2021) e269.
[26] B. Yan, Y. Zhang, C. Liang, B. Liu, F. Ding, Y. Wang, et al., Stem cell-derived exosomes prevent pyroptosis and repair ischemic muscle injury through a novel exosome/circHIPK3/FOXO3a pathway, Theranostics 10 (15) (2020) 6728–6742.
[27] J.P. Hsin, Y. Lu, G.B. Loeb, C.S. Leslie, A.Y. Rudensky, The effect of cellular context on miR-155-mediated gene regulation in four major immune cell types, Nat. Immunol. 19 (10) (2018) 1137–1145.
[28] J. Henao-Mejia, E. Elinav, C. Jin, L. Hao, W.Z. Mehal, T. Strowig, et al., Inflammasome-mediated dysbiosis regulates progression of NAFLD and obesity, Nature 482 (7384) (2012) 179–185.
[29] Z.M. Younossi, M.E. Rinella, A.J. Sanyal, S.A. Harrison, E.M. Brunt, Z. Goodman, et al., From NAFLD to MAFLD: implications of a premature change in terminology, Hepatology 73 (3) (2021) 1194–1198.
[30] T. Qiu, P. Pei, X. Yao, L. Jiang, S. Wei, Z. Wang, et al., Taurine attenuates arsenic-induced pyroptosis and nonalcoholic steatohepatitis by inhibiting the autophagic-inflammasomal pathway, Cell Death Dis. 9 (10) (2018) 946.
[31] S. Gaul, A. Leszczynska, F. Alegre, B. Kaufmann, C.D. Johnson, L.A. Adams, et al., Hepatocyte pyroptosis and release of inflammasome particles induce stellate cell activation and liver fibrosis, J. Hepatol. 74 (1) (2021) 156–167.
[32] R.F. Schwabe, I. Tabas, U.B. Pajvani, Mechanisms of fibrosis development in nonalcoholic steatohepatitis, Gastroenterology 158 (7) (2020) 1913–1928.
[33] J.H. Lee, Y.R. Shim, W. Seo, M.H. Kim, W.M. Choi, H.H. Kim, et al., Mitochondrial Double-Stranded RNA in exosome promotes interleukin-17 production through Toll-Like receptor 3 in alcohol-associated liver injury, Hepatology 72 (2) (2020) 609–625.
[34] M. Shen, Y. Shen, X. Fan, R. Men, T. Ye, L. Yang, Roles of macrophages and exosomes in liver diseases, Front. Med. 7 (2020) 583691.
[35] S. Zhao, Y. Mi, B. Guan, B. Zheng, P. Wei, Y. Gu, et al., Tumor-derived exosomal miR-934 induces macrophage M2 polarization to promote liver metastasis of colorectal cancer, J. Hematol. Oncol. 13 (1) (2020) 156.
[36] M. Babuta, I. Furi, S. Bala, T.N. Bukong, P. Lowe, D. Catalano, et al., Dysregulated autophagy and lysosome function are linked to exosome production by Micro-RNA 155 in alcoholic liver disease, Hepatology 70 (6) (2019) 2123–2141.